Hepatocyte-Targeted Nuclear Imaging Using ^{99m}Tc-Galactosylated Chitosan: Conjugation, Targeting, and Biodistribution

Eun-Mi Kim, MS[1,2]; Hwan-Jeong Jeong, MD, PhD[1,2]; In-Kyu Park, PhD[3]; Chong-Su Cho, PhD[3]; Chang-Guhn Kim, MD, PhD[1,2]; and Hee-Seung Bom, MD, PhD[4]

[1]Department of Nuclear Medicine, Wonkwang University School of Medicine, Iskan, Korea; [2]Wonkwang Institute of Medical Science, Iksan, Korea; [3]School of Agricultural Biotechnology, Seoul National University, Seoul, Korea; and [4]Department of Nuclear Medicine, Chonnam National University School of Medicine, Gwangju, Korea

Galactosyl-methylated chitosan (GMC) is a galactosylated chitosan (GC) that is chemically modified to improve labeling efficiency with ^{99m}Tc compared with native GC. The aim of this study was to investigate the possibility of liver-targeted nuclear imaging with ^{99m}Tc-GMC bound to asialoglycoprotein receptors (ASGP-R). **Methods:** GMC was obtained after the coupling of lactobionic acid, as the galactose moiety, and methyl iodide with chitosan. Using GMC-labeled fluorescein isothiocyanate (FITC-GMC), we examined whether GMC was localized in hepatocytes. After injection via the tail vein of mice with ^{99m}Tc-GMC and galactose-free ^{99m}Tc-methylated chitosan (MC), images were acquired with a γ-camera equipped with a pinhole collimator. Biodistribution was obtained from 10, 60, and 120 min after injection. **Results:** The composition of galactose groups in GC and tri-, di-, and monomethylated GC was confirmed by nuclear magnetic resonance spectroscopy. FITC-GMC was primarily positioned in hepatocytes, and not in Kupffer cells, of the mouse with a scattered pattern. The γ-camera images showed rapid localization of ^{99m}Tc-GMC to liver. The percentage injected doses per gram (%ID/g) of liver were 11.155 ± 2.332, 14.018 ± 6.081, and 14.082 ± 1.670 %ID/g (mean ± SD) at 10, 60, and 120 min after injection, respectively. By contrast, galactose-free ^{99m}Tc-MC accumulated faintly in the liver. **Conclusion:** ^{99m}Tc-GMC specifically localized to the liver except for the kidneys in the mouse. GMC may be used to target the ASGP-R on the hepatocytes for nuclear imaging.

Key Words: ^{99m}Tc; galactosylated chitosan; hepatocyte; target; asialoglycoprotein receptor

J Nucl Med 2005; 46:141–145

The asialoglycoprotein analogs labeled with ^{99m}Tc—^{99m}Tc-diethylenetriaminepentaacetic acid galactosyl neoglycoalbumin (^{99m}Tc-NGA) and ^{99m}Tc-diethylenetriaminepentaacetic acid galactosyl human serum albumin (^{99m}Tc-GSA)—were designed and have been used for the imaging of hepatocytes (*1,2*). The degree of hepatic uptake of these radiopharmaceuticals correlates well with hepatic function. These radiophamaceuticals are known to bind asialoglycoprotein receptors (ASGP-R) that specifically exist on the mammalian polygonal cell surface, situated on the hepatocyte membrane (*1–4*). Because ASGP-R recognize galactose or *N*-acetylgalactosamine residues of desialylated glycoproteins (*5*), materials having these ligands—regardless of whether a monomer or a polymer—have been studied for targeting hepatocytes directly. In the field of bioengineering, polymers and other materials containing ligands such as galactose (*6–8*), apoprotein E (*9*), and lactose (*10*) have been studied to target hepatocytes for delivery of drugs or genes. Recently, several researchers had reported that galactosylated chitosan (GC) binds to hepatocytes due to the galactose residue positioned on chitosan's exterior (*7,8*).

Chitosan, a biodegradable polysaccharide, is composed of 2 subunits: D-glucosamine and *N*-acetylglucosamine. Chitosan interacts strongly with many materials containing a negative charge (e.g., proteins, anionic polysaccharides, nucleic acids, and so forth) and has a large capacity to chelate metal ions (*11–13*). Chitosan derivatives were also thought to chelate with ^{99m}Tc because of the amine group of D-glucosamine. In comparison with other polymer materials, chitosan derivatives have several advantageous qualities: They are biodegradable, relatively nontoxic, biocompatible, and cost-effective and have low immunogenicity (*11,14*).

Because of these properties, GC and its derivatives, which have been used as one of the nonviral vectors for liver-targeted gene delivery, have the potential to be novel nuclear imaging radiopharmaceuticals for targeting hepatocytes. Therefore, we attempted to make suitable materials for labeling with ^{99m}Tc in GC derivatives not reported elsewhere and to use these materials for imaging in a hepatocyte-specific in vivo study.

Received Mar. 30, 2004; revision accepted Jun. 1, 2004.

For correspondence or reprints contact: Hwan-Jeong Jeong, MD, PhD, Department of Nuclear Medicine, Wonkwang University Hospital, 344-2 Sinyong-dong, Iksan, Jellabuk-do, 570-711, Korea.

E-mail: jayjeong@wonkwang.ac.kr

MATERIALS AND METHODS

Materials

Water-soluble chitosan (molecular weight ≈ 5,000, 97% deacetylated) was kindly provided by Dr. Jae-Woon Nah (Sunchon National University, Sunchon, Korea). Fluorescein isothiocyanate (FITC) and stannous chloride dihydrate were purchased from Sigma-Aldrich Co. ^{99m}Tc-Pertechnetate was eluted from a technetium generator (Amersham Health) prepared in our hospital. Instant thin-layer chromatography (ITLC)-SG chromatographic strips were purchased from Gelman Sciences. Female BALB/c mice, 5–6 wk old and weighing 16–18 g (Harlan-Asia, Daehanbiolink, Co. Ltd.), were kept in cages (2 mice per cage) and fed standard laboratory chow and water. All animal experiments were approved by the Wonkwang University School of Medicine Committee and were performed in accordance with their guidelines.

Synthesis of GC and Galactosyl-Methylated Chitosan (GMC)

Chitosan was coupled with lactobionic acid (LA) (Tokyo Chemistry Industry) via an active ester intermediate using 1-ethyl-3-(3-dimethylaminopropyl)carbodiimide hydrochloride (EDC) (Dojindo) and *N*-hydroxysuccinimide (NHS) (Pierce Chemicals) (*15*). Chitosan and equivalent moles of LA were dissolved in 10 mmol/L *N*,*N*,*N*′,*N*′-tetramethylethylenediamine/HCl buffer solution (pH 4.7). EDC and NHS were added to this solution and stirred for 72 h at room temperature. The resulting GC was dialyzed for 4 d using a Spectra/Por7 membrane (molecular weight cutoff = 3,500; Spectrum) against distilled water. After dialysis, GC was freeze-dried.

After 0.1 g of GC and 0.24 g of sodium iodide were dissolved in 4 mL of *N*-methyl-2-pyrrolidone (NMP) at 60°C, 0.55 mL of a 15% aqueous sodium hydroxide solution and 0.6 mL of methyl iodide were added and then reacted for 1 h with stirring (*16,17*). The product was isolated by precipitation with ethanol and subsequent centrifugation. To exchange the counterion iodide with chloride, the product was dissolved in 5 mL of 10% NaCl aqueous solution and precipitated with ethanol, isolated by centrifugation, and thoroughly washed with ethanol and ether. The final product was dried in a vacuum and measured for the degree of methylation by ^{1}H nuclear magnetic resonance (NMR). ^{1}H NMR spectra were measured in deuterated water, using a 600-MHz spectrometer (Bruker).

Conjugation of GMC with FITC

GMC was dissolved in sodium bicarbonate buffer (0.2 mol/L, pH 9.0). FITC (10 mg/mL in *N*,*N*-dimethylformamide) was slowly added to the buffer. The mixture was gently stirred at room temperature for 4 h. FITC-GMC was precipitated with ethanol and dried in a vacuum.

Radiolabeling with ^{99m}Tc

GMC was dissolved in distilled water (1 μg/μL). Stannous chloride was dissolved in 0.02N HCl (0.2 μg/μL, w/v). One hundred microliters of GMC were mixed with 10 μL stannous chloride solution in a vial at room temperature. Labeling was performed by adding 111 MBq ^{99m}Tc-sodium pertechnetate (0.3 mL saline) to this mixture. The final volume of the solution was brought to 1 mL with saline and then shaken gently. The pH of the final mixture was ~7.0. The mixture was allowed to react for a further 30 min, with occasional shaking. Labeled GMC was then filtered through a 0.22-μm filter (Millipore) and the filter was washed with saline. Labeling efficiency was determined using ITLC-SG strips with saline and acetone as the mobile phase at 15 and 60 min after filtering.

Imaging and Biodistribution Studies

After injection of 18.5 MBq ^{99m}Tc-GMC (200 μL containing 0.47 μmol GMC) and 18.5 MBq ^{99m}Tc-methylated chitosan (MC) (200 μL containing 0.5 μmol MC) via the tail vein of mice, dynamic and static images were performed with a γ-camera (Vertex; ADAC Laboratories) with a 5-mm pinhole collimator, window setting of 140 keV, and 20% width. γ-Camera images were acquired at 10, 60, and 120 min after injection. The static images were stored in a 512 × 512 matrix size and acquisition times were 120 s. Regions of interest in the liver and heart were drawn and time–activity curves were acquired. Animals were killed and each organ was dissected at 10, 60, and 120 min after injection (n = 5). Dissected tissue samples were rinsed of excess blood, weighed, and counted in a γ-counter. The biodistribution of ^{99m}Tc-GMC in each organ was calculated as a percentage of the injected dose per gram of tissue (%ID/g). The total counts injected per animal were calculated by the difference between the original syringe counts and the remaining syringe counts after injection. Correction was made for background radiation and physical decay during counting.

Uptake of FITC-GMC by Hepatocytes

Mice were sedated with a mixture of ketamine (100 mg/kg) and xylazine (10 mg/kg) administered intraperitoneally, and FITC-GMC was injected via the tail vein. To differentiate hepatocytes and Kupffer cells, India ink was injected via the tail vein in 1 mouse and FITC-GMC and India ink were injected systemically in the other mouse. Mice were sacrificed after 30 min, and the liver was isolated and embedded in 50% (v/v) optimal cutting compound (OCT; Sakura Finetek). Cryosections were cut at 6 μm using a microtome (Leica) and placed onto slides. The slides were dipped in acetone and then washed with phosphate-buffered saline. Fluorescence was visualized using a Zeiss Axioskop2 optical microscope. Green fluorescence was observed using the 450- to 490-nm excitation filter. The images were recorded by using Zeiss AxioVision software.

RESULTS

Synthesis of GMC

The synthetic scheme for GMC is outlined in Figure 1. Figure 2A shows NMR spectra of GC. The substitution value of galactose in GC was calculated by comparing the characteristic peak areas of the galactose group (4.1 ppm) with that of the 2.0-ppm peak attributed to the original acetamide group of chitosan. The substitution value of LA coupled with chitosan in GC was estimated to be 7.42 mol%. Figure 2B shows a peak at 2.2 ppm assigned to $NH(CH_3)$, 3.1 ppm assigned to $N(CH_3)_3^+$, and 3.4 ppm assigned to $N(CH_3)_2$. The composition of tri-, di-, and monomethylation of GC was 8.8, 46.0, and 35.2 mol%, respectively.

Radiolabeling with ^{99m}Tc

The radiolabeling efficiency of ^{99m}Tc-GC was increased >95% by incorporation of methyl groups and that lasted up

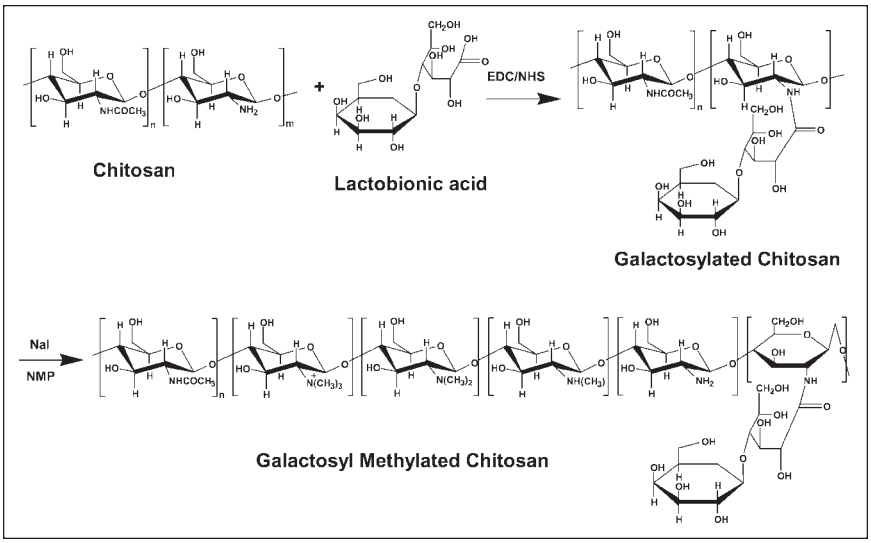

FIGURE 1. Schematic structures of GC and GMC.

to 1 h. As shown in Figure 3, the labeling stability is preserved by methylation. The labeling efficiency determined by ITLC-SG in acetone was at least 98% at 6 h in the case of ^{99m}Tc-MC and was >95% at 6 h in the case of ^{99m}Tc-GMC (data not shown). ^{99m}Tc-GMC was incubated at 37°C with 1 mL of human serum. The result of human serum stability was >81% during 2 h.

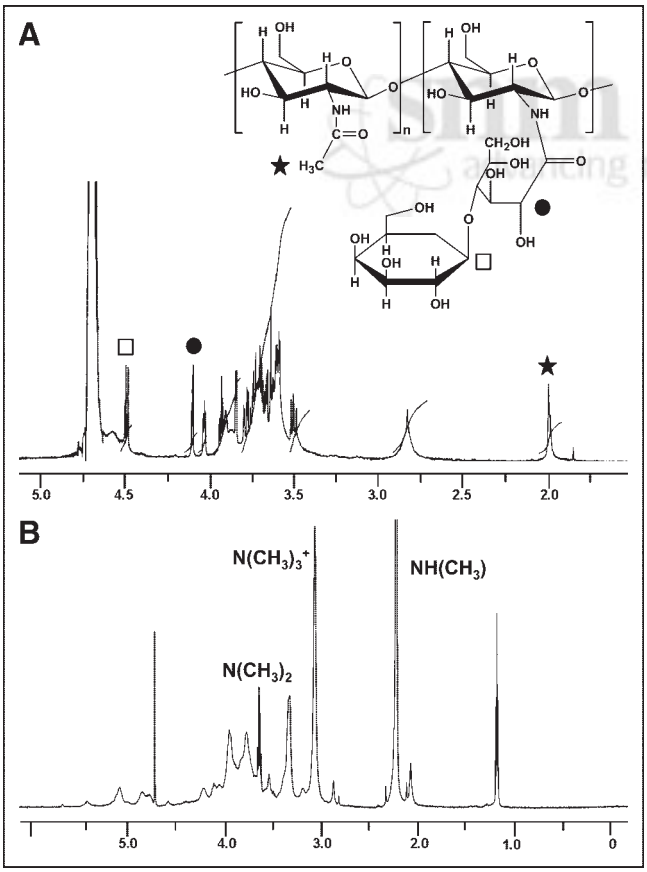

FIGURE 2. ^{1}H NMR spectra of GC (A) and GMC (B). Solid star, open square, and solid circle correspond to proton of acetamide group of chitosan (δ 2.0 ppm), proton attached at C2 in grafted galactose group (δ 4.5 ppm), and proton attached at C2 in opened pyranose ring linked between grafted galactose group and chitosan main chain (δ 4.2 ppm), respectively.

Imaging and Biodistribution Studies

The distributions of ^{99m}Tc-MC and ^{99m}Tc-GMC in mice are illustrated in Figures 4A and 4B. ^{99m}Tc-GMC was transported to the liver within a few minutes of injection, whereas some faint liver uptake occurred in ^{99m}Tc-MC–injected mice. The pattern of liver uptake was markedly different between the 2 materials because of the galactose residue positioned on chitosan's exterior. The liver activity of ^{99m}Tc-GMC gradually increased until 2 h (Fig. 4C). The calculations for the biodistribution of the ^{99m}Tc-GMC are summarized in Table 1. The values of %ID/g of liver were as follows: 11.155 ± 2.332, 14.018 ± 6.081, and 14.082 ± 1.670 %ID/g (mean ± SD) at 10, 60, and 120 min after injection, respectively. ^{99m}Tc-GMC also showed high activity in the kidney: 27.274 ± 3.061, 21.986 ± 5.108, and 19.615 ± 1.491 %ID/g (mean ± SD).

Uptake of FITC-GMC by Hepatocytes

As shown in Figure 5D, the fluorescence of the liver tissue of mice injected with FITC-GMC was visualized as scattered green-colored spots, in contrast with control liver tissue. No fluorescence was observed in the control liver tissue (Fig. 5B). When injected with India ink only, Kupffer cells appeared to be black, spindle-shaped cells under light and were shown as small fluorescent points under the 450- to 490-nm excitation filter (Figs. 5B and 5D). When injected with both FITC-GMC and India ink systemically, the fluorescent image showed larger spots or clusters in the space between Kupffer cells in addition to fluorescent points that were positioned in Kupffer cells under 10× magnification (Fig. 5D, arrows). These results suggest that accumulation of GMC in the liver was mediated by the ASGP-R.

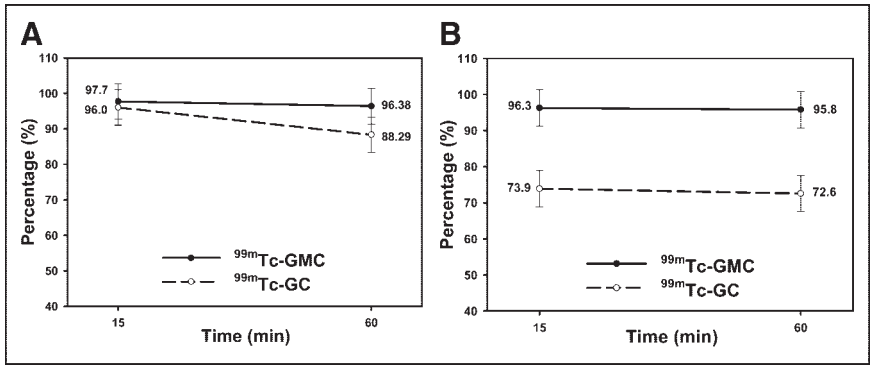

FIGURE 3. Labeling efficiency of ^{99m}Tc-GC and ^{99m}Tc-GMC in saline (A) and acetone (B).

DISCUSSION

Hepatocytes are the most abundant type of liver cell. Also in the liver are biliary epithelial cells, hepatic stellate cells, and littoral cells such as Kupffer cells (*18*). Nuclear medicine has followed 2 major approaches for estimating liver function. One approach to estimating liver disease is colloid scintigraphy, which indirectly evaluates liver function on the basis of Kupffer cell removal (*19*). The other approach is a direct evaluation using, for example, ^{99m}Tc-GSA, which binds to ASGP-R and is well correlated with hepatic function (*1,19*). Although GSA is a radiolabeled serum albumin against the ASGP-R and has been evaluated in clinical studies for imaging, ^{99m}Tc-GSA scintigraphy is not yet fully accepted in the field (*4*). Recent studies with chitosan coupled to LA showed that it was recognized by ASGP-R of hepatocytes and taken up by ASGP-R–mediated endocytosis (*7,8*). We chose a water-soluble chitosan as the imaging agent, with this chitosan conjugated to LA. Water-soluble chitosan has useful characteristics, such as being biocompatible, biodegradable, nonimmunogenic, and cleared very rapidly from the bloodstream (*11,20*). Our results indicate that ^{99m}Tc-GMC exhibited fast clearance that was dominated by rapid excretion through the kidney. This suggests water-soluble chitosan as a good polymeric imaging carrier that overcomes accumulation in the body. Moreover, the easy and inexpensive availability of chitosan could be beneficial for applications in scintigraphic imaging.

In this study, we succeeded in performing hepatocyte-targeted nuclear imaging using ^{99m}Tc-GMC in mice. Under the hypothesis that secondary and tertiary amines of chitosan can donate lone pairs of electrons to form coordinate covalent bonds with ^{99m}Tc by methylation, we proposed to achieve liver imaging of mice with higher labeling efficiency using ^{99m}Tc-GMC versus ^{99m}Tc-GC (Fig. 3). Functional groups such as $–COO^–$, $–OH^–$, $–NH_2$, and –SH can form coordinate covalent bonds with ^{99m}Tc (*18,21*), with the amino group of chitosan specifically serving as a chelating moiety. However, labeling yield is expected to be low, especially for highly deacethylated chitosan, because protonation of the amine group on dissolution at acidic and neutral pH ($pK_a = 6.5$) causes chitosan to behave as a linear polyelectrolyte (*11*). Methylation of chitosan has been studied for improving solubility at physiologic pH. The synthetic procedures are well defined, and Le Dung et al. (*16*) and Sieval et al. (*17*) have described the preparation. In the present study, GC was modified to GMC, which was intended to increase both the hydrophilicity of the chitosan and the labeling efficiency with ^{99m}Tc.

In our study, ^{99m}Tc-GMC was highly specific for the ASGP-R using FITC-GMC, which was distributed diffusely in hepatocytes. These results are consistent with previous data obtained in gene delivery research that involved chitosan coupled with LA bearing a galactose moiety. As shown in Figure 4, the highest levels of the radiotracer were

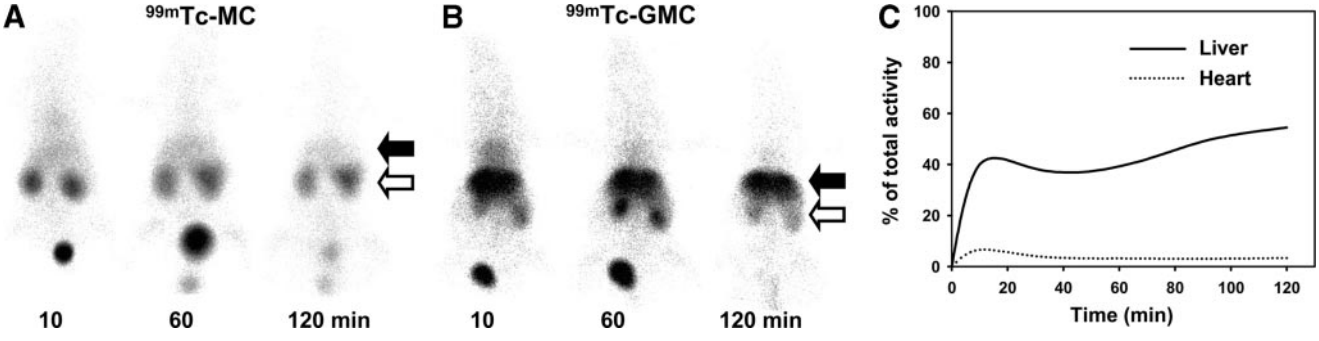

FIGURE 4. γ-Camera images of mice at 10, 60, and 120 min after injection of ^{99m}Tc-MC (A) and ^{99m}Tc-GMC (B). After ^{99m}Tc-GMC injection into mice, ^{99m}Tc-GMC was specifically localized to liver (B), but ^{99m}Tc-MC uptake was faint (A). Solid arrows point to liver; open arrows indicate kidneys of each animal. (C) Time–activity curves of liver and heart of mouse injected with ^{99m}Tc-GMC.

TABLE 1
Biodistribution of ^{99m}Tc-GMC in BALB/c Mice

Organ	%ID/g		
	10 min* (n = 5)	60 min* (n = 5)	120 min* (n = 5)
Blood	8.642 ± 1.917	1.769 ± 0.705	3.362 ± 0.774
Intestine	0.869 ± 0.317	1.640 ± 1.633	1.975 ± 2.043
Liver	11.155 ± 2.332	14.018 ± 6.081	14.082 ± 1.670
Spleen	4.264 ± 1.726	4.271 ± 1.057	3.821 ± 0.221
Stomach	0.869 ± 0.320	0.669 ± 0.446	0.863 ± 0.165
Heart	1.664 ± 0.321	0.685 ± 0.094	1.031 ± 0.277
Lung	3.676 ± 0.770	1.855 ± 1.430	2.119 ± 0.246
Bone	1.545 ± 1.245	1.521 ± 0.956	1.482 ± 0.231
Muscle	0.539 ± 0.082	0.295 ± 0.128	0.249 ± 0.071
Kidney	27.274 ± 3.061	21.986 ± 5.108	19.615 ± 1.491

*Time after injection of radioconjugate.
Values are mean ± SD.

found in the kidneys. The high kidney activity likely resulted from the particular characteristics of water-soluble chitosan (*20*). Some renal activity detected in ^{99m}Tc-MC–injected mice likely came about for the same reason. The biodistribution of ^{99m}Tc-GMC was investigated at 10, 60, and 120 min after intravenous injection in mice (Table 1). Higher activity in the liver and kidney was observed; higher liver activity gradually increased up to 2 h, whereas kidney uptake decreased over time.

CONCLUSION

^{99m}Tc-GMC is specifically localized in the liver, binding to the ASGP-R on hepatocytes. This study shows that ^{99m}Tc-GMC is capable of efficiently imaging the liver in an animal model.

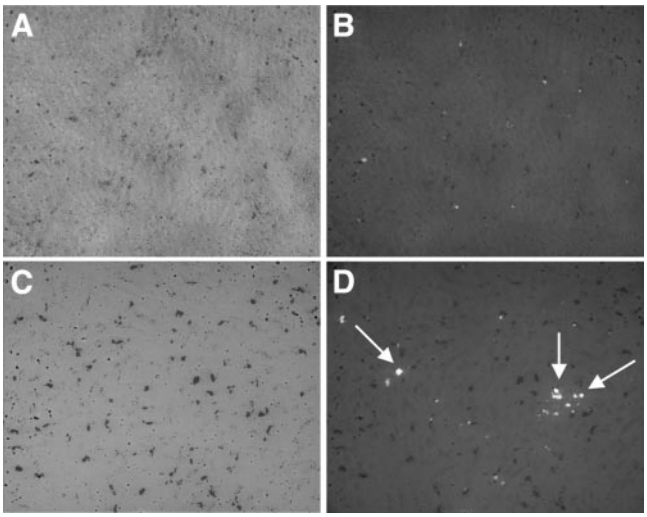

FIGURE 5. (A and C) Light microscope images of liver tissue. (B and D) Fluorescence images of liver tissue. India ink trapped by Kupffer cells appears as black spots in A–D. Fluorescence of B was from India ink. Fluorescence from FITC-GMC was different from that of India ink trapped in Kupffer cells (D). Arrows indicate fluorescence of FITC-GMC combined with hepatocytes.

ACKNOWLEDGMENTS

The authors acknowledge the efforts of the technologists of the Department of Nuclear Medicine in Wonkwang University Hospital for animal care and technical assistance preparing γ-camera images. This work was supported by grant M20203200028-02A0702-00411 of the Nuclear Energy Research and Development Program from the Ministry of Science and Technology of Korea.

REFERENCES

1. Kudo M, Ikekubo K, Todo A, et al. Hepatic receptor imaging with ^{99m}Tc GSA: estimates of liver function in acute liver disease. *Nippon Shokakibyo Gakkai Zasshi.* 1992;89:616–626.
2. Stadalnik RC, Vera DR, Woodle ES, et al. Technetium-99m NGA functional hepatic imaging: preliminary clinical experience. *J Nucl Med.* 1985;26:1233–1242.
3. Wagner HN, Szabo Z, Buchanan JW. *Principles of Nuclear Medicine*. 2nd ed. Philadelphia, PA: WB Saunders; 1995.
4. Yasuharu O, Haruo I, Akira H, et al. The mean transit time and functional image in asialoglycoprotein receptor scintigraphy: a novel modality for evaluating the regional dynamic function of hepatocytes. *J Nucl Med.* 2002;43:1611–1615.
5. Pricer WE, Ashwell G. The binding of desialylated glycoproteins by plasma membranes of liver. *J Biol Chem.* 1971;246:4825–4833.
6. Zanta MA, Boussif O, Adib A, Behr JP. In vivo gene delivery to hepatocytes with galactosylated polyethylenimine. *Bioconjug Chem.* 1997;8:839–844.
7. Park IK, Kim TH, Park YH, et al. Galactosylated chitosan-graft-poly(ethylene glycol) as hepatocyte-targeting DNA carrier. *J Control Release.* 2001;76:349–362.
8. Park IK, Yang J, Jeong HJ, et al. Galactosylated chitosan as a synthetic extracellular matrix for hepatocytes attachment. *Biomaterials.* 2003;24:2331–2337.
9. Rensen PC, Herijgers N, Netscher MH, et al. Particle size determines the specificity of apolipoprotein E-containing triglyceride-rich emulsions for the LDL receptors versus hepatic remnant receptor in vivo. *J Lipid Res.* 1997;38:1070–1084.
10. Choi YH, Liu F, Park JS, et al. Lactose-poly-(ethylene glycol)-grafted poly-L-lysine as hepatoma cell targeted gene carrier. *Bioconjug Chem.* 1998;9:708–718.
11. Sandford P. Chitosan: commercial uses and potential applications. In: Skjåkbraek G, Anthonsen T, Sandford P, eds. *Chitin and Chitosan.* London, UK: Elsevier Applied Science; 1989:51–69.
12. Muzzarelli RAA, Rocchetti R. Enhanced capacity of chitosan for transition-metal ions in sulphate-sulphuric acid solutions. *Talanta.* 1974;21:1137–1143.
13. Muzzarelli RAA. *Chitin.* Oxford, UK: Pergamon; 1977.
14. Rao SB, Sharma CP. Use of chitosan as a biomaterial: studies on its safety and hemostatic potential. *J Biomed Mater Res.* 1997;34:21–28.
15. Sehgal D, Vijay IK. A method for the high efficiency of water-soluble carbodiimide-mediated amidation. *Anal Biochem.* 1994;218:87–91.
16. Le Dung P, Milas M, Rinaudo M, Desbrières J. Water soluble derivatives obtained by controlled chemical modifications of chitosan. *Carbohydr Polymers.* 1994;24:209–214.
17. Sieval AB, Thanou M, Kortze AF, Verhoel JC, Brussee J, Junginger HE. Preparation and NMR characterization of highly substituted N-trimethyl chitosan chloride. *Carbohydr Polymers.* 1998;36:157–165.
18. Saha GB. *Fundamentals of Nuclear Pharmacy.* 4th ed. New York, NY: Springer-Verlag; 1998.
19. Sasaki N, Shiomi S, Iwata Y, et al. Clinical usefulness of scintigraphy with ^{99m}Tc-galactosyl-human serum albumin for prognosis of cirrhosis of the liver. *J Nucl Med.* 1999;40:1652–1656.
20. Onishi H, Machida Y. Biodegradation and distribution of water-soluble chitosan in mice. *Biomaterials.* 1999;20:175–182.
21. Arano Y. Delivery of diagnostic agents for gamma-imaging. *Adv Drug Deliv Rev.* 1999;37:103–120.